

Thermodynamic Modeling of Aqueous Polyelectrolyte Solutions with Mixed-valent Counterions

Yuan Li, Chau-Chyun Chen*

Department of Chemical Engineering, Texas Tech University, Lubbock, TX 79409-3121, USA

* Corresponding author. Tel.: +1 806.834.3098. Email address: chauchyun.chen@ttu.edu

ORCID: Chau-Chyun Chen: 0000-0003-0026-9176

Abstract

Thermodynamic modeling of aqueous polyelectrolyte solutions with salts is of significant interest for many industrial applications. This study applies the polyelectrolyte Nonrandom Two-liquid activity coefficient model to aqueous polyelectrolyte solutions with mixed-valent counterions. A modified Delocalized Binding Theory was proposed to determine the polyion condensation fractions of the mixed counterions. This modified theory accounts for the electrostatic binding of the counterions on the polyion, the dissociation entropy of the counterions, and the electrostatic interaction between the uncondensed ionic species. Given the polyion condensation fractions, the critical value of Manning's parameter ξ and the amounts of uncondensed polyions and counterions can be calculated along with the activity coefficients of mobile ions. The model successfully correlates experimental data for various aqueous polyelectrolyte systems with mixed-valent counterions.

Keywords: aqueous polyelectrolyte solutions; counterion condensation; delocalized binding theory; polyelectrolyte NRTL model; mixed-valent counterions

1. Introduction

Much progress has been made in the thermodynamic modeling of aqueous polyelectrolyte solutions in the past decades [1-4]. Among them, Manning's limiting law [4], which is derived from statistical thermodynamics by integrating electrostatic interactions between point charges and rod-like charged polyion backbone chains, is the most remarkable achievement. However, while Manning's limiting law has been successfully applied to elucidate thermodynamic properties of dilute aqueous polyelectrolyte solutions, the limiting law is inadequate to represent the thermodynamic properties of polyelectrolytes with high salt concentrations and it fails for the limiting cases of aqueous salt solutions without polyelectrolytes [5-7]. This deficiency hampers the application of Manning's limiting law in wider applications such as the treatment of brine solutions with ion-exchange membranes. To overcome the inadequacy of Manning's limiting law in high salt concentration solutions, Yu *et al.* [6, 7] proposed a polyelectrolyte Nonrandom Two-liquid (NRTL) activity coefficient model by extending Manning's limiting law with two additional terms: the Pitzer-Debye-Hückel term [8] to account for the long-range electrostatic interactions between uncondensed ionic species and the local composition term derived from the electrolyte NRTL (eNRTL) model [9, 10] to account for the short-range van der Waals molecule-molecule, molecule-ion, and ion-ion interactions. The polyelectrolyte NRTL model has been successfully applied to quantitatively correlate the thermodynamic properties of aqueous polyelectrolyte solutions with either monovalent or multivalent counterions [6, 7]. In addition, the model has been successfully applied to elucidate the partitioning of mobile ions between ion-exchange membranes and external brine solutions [11]. However, as industrial electrolyte solutions often involve multiple ions with mixed charge

valences, it is necessary to examine the applicability of the polyelectrolyte NRTL model for aqueous polyelectrolyte solutions with mixed-valent counterions.

As a critical step in thermodynamic modeling of aqueous polyelectrolyte solutions, counterion condensation in polyelectrolyte solutions must be taken into account. A unique phenomenon in aqueous polyelectrolyte solutions, counterions condense on the polyion chain to reduce the charge density of the polyion chain below a critical value. Manning's limiting law defines Manning's parameter ξ as the dimensionless charge density of the polyion chain. For an aqueous polyelectrolyte solution with a single type of counterion, counterion condensation should take place if ξ is greater than the critical value of $1/|z_i z_p|$, where z_i and z_p are the valences of counterion and polyion segments, respectively. However, the way to determine the critical ξ value in the case of mixed-valent counterions was not clear. Initially Manning tackled this question [12] by following a step-by-step condensation sequence for systems with both monovalent and divalent counterions. He suggested that divalent counterions should condense first until either the critical ξ value of $1/2$ is reached or the divalent counterions are depleted. Subsequently, monovalent counterions should condense until the critical ξ value of unity is reached. However, this condensation scenario failed to explain the experimental data [12]. Later, Manning presented his Delocalized Binding Theory (DBT) [13] for counterion condensation in polyelectrolyte solutions with mixed-valent counterions. DBT hypothesizes that the polyion condensation fractions of counterions should reflect the minimal Gibbs energy of the condensed system, as determined from the electrostatic interactions of and the entropy of mixing the charged polyions and counterion species. Readily reduced to the counterion condensation scenario for single-counterion polyelectrolyte systems, DBT provides a sound theoretical foundation for the determination of counterion condensation for aqueous polyelectrolyte

solutions with mixed-valent counterions. Also called “Two-Variable Theory”, DBT was originally proposed to predict polyion condensation fractions for binary counterion systems with one monovalent and one divalent counterions. Several studies have subsequently applied Manning’s limiting law incorporating “Two-Variable Theory” for counterion condensation to represent aqueous polyelectrolyte solutions with mixed-valent counterions at low concentrations [14-17].

This study extends the polyelectrolyte NRTL model for aqueous polyelectrolyte solutions with mixed-valent counterions. To be consistent with the assumptions of polyelectrolyte NRTL model, DBT is formulated for multiple counterions and further modified with an additional long-range electrostatic ion-ion interactions term taken from the Pitzer-Debye-Hückel theory [18]. The polyelectrolyte NRTL model is then applied to correlate experimental data of aqueous polyelectrolyte solutions including polystyrene sulfonate (PSS), polymethyl acrylate (PMA), and dextran sulfate (DS) with mixed-valent counterions. The experimental data include the polyion condensation fractions (θ_i) and the ionic activity coefficient (γ_i) of counterions.

2. Thermodynamic Framework

2.1. Delocalized Binding Theory

Upon counterion condensation, the charge density ξ of the polyion chain is reduced to a value of $(1 - \sum_i^{n_{ct}} |z_i| \theta_i) \xi$, where i is the index of counterion type, n_{ct} is the total number of counterion types, z_i is the valence of counterion type i , and θ_i is the polyion condensation fraction of counterion type i representing the number of counterion condensed per polyion segment or the ratio of the number of counterion i condensed ($N_i^{condensed}$) and the number of polyion segment ($N_{p,0}$), (i.e., $\theta_i = N_i^{condensed} / N_{p,0}$).

Derived for the limiting case of counterion concentration approaching zero, DBT [13] states that θ_i , the polyion condensation fraction of counterion i , is determined by the minimization of the Gibbs energy of counterion condensation with respect to the polyion condensation fractions θ_i . This equilibrium state of incomplete binding “representing the balance between maximization of entropy by dissociation and minimization of energy by binding.” Here the Gibbs energy of counterion condensation is composed of the contribution from electrostatic binding of the counterions on the polyion (g^{el}) and the contribution from dissociation entropy (g^{mix}). The g^{el} term represents the energy required to charge the polyion chain up to the charge density after counterion condensation. The g^{mix} term represents the translational entropy for condensing a specific amount of counterions from the bulk solution to the surface of the polyion.

$$\frac{\partial(g^{el} + g^{mix})}{\partial\theta_i} = 0 . \quad (1)$$

Derived from the linearized Poisson-Boltzmann equation with cylindrical coordinates, the expression for g^{el} [13] shown below has been generalized for an aqueous polyelectrolyte solution with the polyion charge density ξ , the polyion segment molality $m_{p,0}$, the number of counterion types n_{ct} , the counterion ion i molality $m_{i,0}$, and the number of kg of solvent water n_w [13]:

$$g^{el} = \frac{G^{el}}{n_w RT} = -\xi m_{p,0} \left(1 - \sum_i^{n_{ct}} |z_i| \theta_i \right)^2 \ln(\kappa b) , \quad (2)$$

$$\xi = \frac{q_e^2}{\epsilon k T b} , \quad (3)$$

$$\kappa^2 = \frac{4\pi q_e^2 N_A d_w}{1000 \epsilon k T} \sum_i^{n_t} z_i^2 m_i , \quad (4)$$

where q_e is the elementary charge, ϵ is the dielectric constant of the aqueous media, k is the Boltzmann constant, T is the temperature, b is the distance between each functional group on polyelectrolyte, N_A is the Avogadro's constant, d_w is the density of water, n_t is the total number of mobile ion types, and m_i is the concentration of the uncondensed mobile ion i in the solution. Note that, for counterions, $m_i = m_{i,0} - \theta_i m_{p,0}$; for coions $m_i = m_{i,0}$.

Derived from the entropy change resulting from the counterion condensation [13], the following expression for g^{mix} has been generalized for systems with n_{ct} number of counterion types:

$$g^{mix} = \frac{G^{mix}}{n_w RT} = m_{p,0} \sum_i^{n_{ct}} \left[\theta_i \ln \left(\frac{\theta_i / V_p}{m_i} \right) \right] , \quad (5)$$

here V_p is the volume of the “association region” per mole of polyion segment wherein counterions are “bound” to the polyion chain. V_p is a function of the polyion charge density ξ , the counterion concentration m_i , the counterion charge number z_i , and the distance between each functional group on polyion chain b [13].

Figure 1 shows the Gibbs energy contour plot with varying polyion condensation fractions of monovalent counterion 1 and divalent counterion 2. The polyelectrolyte ξ value is fixed at 2.5, the polyion segment concentration is 0.01 molal, and the monovalent and divalent counterion concentrations are both fixed at 0.01 molal. Figure 1a shows that the Gibbs energy of the system is minimized at $\theta_1 = 0.152$, and $\theta_2 = 0.319$. Figure 1b shows that g^{el} favors counterion condensation because the electrostatic potential between the polyion and mobile ion

drops as the polyion is neutralized by counterions, and g^{el} decreases with the increase in polyion condensation fractions. On the other hand, Figure 1c shows that g^{mix} disfavors counterion condensation because counterion condensation yields a lower degree of randomness for the system, and g^{mix} increases with the increase in polyion condensation fractions.

The Gibbs energy minimization calculation is further conducted for the same polyelectrolyte ($m_{p,0} = 0.01$ molal, $\xi = 2.5$) but with counterion concentrations ten times higher. Figure S1a shows the total Gibbs energy contour plot for both monovalent and divalent counterion concentrations fixed at 0.1 molal. For the higher salt concentration solution, the minimum Gibbs energy point is at $\theta_1 = 0.279$ and $\theta_2 = 0.327$. Although Figure S1b shows the profile of g^{el} remains similar to the lower concentration case shown in Figure 1b, the profile of g^{mix} changes significantly and Figure S1c shows a minimum point of $\theta_1 = 0.206$ and $\theta_2 = 0.198$.

2.2. Modified Delocalized Binding Theory

Derived for the limiting case of counterion concentration approaching zero, DBT omits the Gibbs energy contribution from the electrostatic potential due to the interactions between the point charge species in the solution. The additional Gibbs energy contribution is captured with the ion-ion interactions term from the Pitzer-Debye-Hückel equation, g^{PDH} . Therefore, the Gibbs energy of counterion condensation, Eq. 1, is expanded to include g^{PDH} in the search of polyion condensation fractions for each counterion i , θ_i :

$$\frac{\partial(g^{el} + g^{mix} + g^{PDH})}{\partial\theta_i} = 0 . \quad (6)$$

The Gibbs energy expression of g^{PDH} is given below [18]:

$$g^{PDH} = \frac{G^{PDH}}{n_w RT} = -A_\phi \frac{4I}{\rho} \ln(1 + \rho\sqrt{I}) , \quad (7)$$

$$A_\phi = \frac{1}{3} \left(\frac{2\pi N_A d_w}{1000} \right)^{\frac{1}{2}} \left(\frac{q_e^2}{\epsilon k T} \right)^{\frac{3}{2}}, \quad (8)$$

$$I = \frac{1}{2} \sum_i^n (z_i^2 m_i), \quad (9)$$

where A_ϕ is the Debye-Hückel constant for the osmotic coefficient, ρ is the closest approach, I is the ionic strength of the solution, and n is the total number of ionic species, including polyion segments.

The Gibbs energy contour plot generated with the modified Delocalized Binding Theory (mDBT) is shown in Figure S2 for a polyelectrolyte solution with $\xi = 2.5$ and $m_{p,0} = 0.01$ molal. The monovalent and divalent counterion concentrations are both fixed at 0.01 molal. Figure S2a shows the minimum Gibbs energy is achieved with $\theta_1 = 0.164$ and $\theta_2 = 0.291$, slightly different from the DBT results shown in Figure 1a. Figure S2b shows g^{PDH} disfavors counterion condensation and g^{PDH} increases with the increase in polyion condensation fractions.

The contribution of g^{PDH} is more pronounced in higher salt concentration cases. Figure S3 shows the Gibbs energy contour plot with both monovalent and divalent counterion concentrations of 0.1 molal. Figure S3a shows the minimum Gibbs energy is achieved at $\theta_1 = 0.315$ and $\theta_2 = 0.166$, significantly different from the minimum suggested by DBT as shown in Figure S1a. Figure S3b shows g^{PDH} disfavors counterion condensation and the absolute g^{PDH} values increase much for the high salt concentration case than the low salt concentration case shown in Figure S2b.

2.3. Polyelectrolyte NRTL Model

As reported in our previous papers [6, 7], there are three contributions to the polyelectrolyte NRTL model: the Manning term (M) [4], the Pitzer-Debye-Hückel term (PDH)

[8], and the local composition term (lc) from the eNRTL model [9, 10]. The Manning term and PDH term represent the long-range polyion-ion electrostatic interactions contribution and the long-range ion-ion electrostatic interactions contribution, respectively. The lc term represents the short-range van der Waals interactions between any species and their first-shell neighboring species subject to the constraints of local electroneutrality and like-ion repulsion. The overall expression of the counterion activity coefficient is:

$$\ln \gamma_i^{polyeNRTL} = \ln \gamma_i^M + \ln \gamma_i^{PDH} + \ln \gamma_i^{lc} . \quad (10)$$

The general expression of Manning term for ionic activity coefficient is shown below [4]:

$$\ln \gamma_i^M = -\frac{1}{2} \left(1 - \sum_j^{n_{ct}} |z_j| \theta_j \right)^2 \xi m_{p,0} \frac{z_i^2}{\sum_{i=1}^{n_t} m_i z_i^2} , \quad (11)$$

here m_i refers to the concentration of counterion ion i after condensation, and it is equal to the initial concentration of counterion i in the solution subtracted by the condensed fraction, i.e., $m_i = m_{i,0} - \theta_i m_{p,0}$. The coion concentration, on the other hand, remains the same as its initial value.

The general expression of the activity coefficient shown in Eq. 11 is readily reduced to the specific expressions used in our previous works for polyelectrolyte solutions with single counterions [6, 7]. For instance, consider a polyelectrolyte solution with counterion Na^+ and coion Cl^- , charge density $\xi < 1$, and no condensation, i.e., $\theta_{\text{Na}^+} = 0$. Eq. 11 reduces to:

$$\ln \gamma_i^M = -\frac{1}{2} \xi m_{p,0} \frac{z_i^2}{m_{\text{Na}^+,0} + m_{\text{Cl}^-,0}} , \quad (12)$$

$$\ln \gamma_{\text{Na}^+}^M = -\frac{1}{2} \xi m_{p,0} \frac{1}{(m_{\text{Na}^+,0} + m_{\text{Cl}^-,0})} , \quad (13)$$

$$\ln \gamma_{Cl^-}^M = -\frac{1}{2} \xi m_{p,0} \frac{1}{(m_{Na^+,0} + m_{Cl^-,0})} . \quad (14)$$

The counterions come from two sources: the dissociation of polyelectrolyte and added salt, i.e., $m_{Na^+,0} = m_{p,0} + m_{salt}$, and coion comes from the added salt only, i.e., $m_{Cl^-} = m_{salt}$. Rewriting Eqs. 13 and 14 in the form of ξ and X (the concentration ratio of polyion segment to added salt, i.e., $X = m_{p,0}/m_{salt}$):

$$\ln \gamma_{Na^+}^M = -\frac{1}{2} \xi \frac{X}{(X+2)} , \quad (15)$$

$$\ln \gamma_{Cl^-}^M = -\frac{1}{2} \xi \frac{X}{(X+2)} . \quad (16)$$

Eqs. 15 and 16 are identical to the equations used in the previous work on modeling of polyelectrolyte solutions with monovalent counterions [6]. The derivation for polyelectrolyte solutions with divalent counterions is similar, and the final expression has been given in the paper on modeling of polyelectrolyte solutions with multivalent counterions [7]. The expressions of the PDH term and lc term of the polyelectrolyte NRTL model for polyelectrolyte solutions with mixed counterions are also the same as those shown in previous publications [6, 7].

Summarized in Table 1, the model parameters include Manning's parameter ξ per polyelectrolyte and two asymmetric eNRTL binary interaction parameters τ_{ij} ($\tau_{ij} \neq \tau_{ji}$) per water-electrolyte pair and per electrolyte-electrolyte pair sharing a common anion. Note that electrolytes in this work can be simple electrolytes such as alkali halides or ion pairs involving polyion charged segments and counterions. The binary interaction parameters for water-electrolyte pairs are readily available in the literature for most aqueous single electrolyte solutions [9, 10]. The binary interaction parameters for the electrolyte-electrolyte pairs are typically set to zero unless high concentrations of electrolytes are involved.

3. Literature Experimental data

Table 2 presents a summary of the literature experimental data available for mixed-valent polyelectrolyte solutions [14-17, 19]. These include data for the polyion condensation fractions (θ_i) and activity coefficients (γ_i) of aqueous polyelectrolyte solutions with mixed mono- and divalent counterions. The polyelectrolyte types include dextran sulfate (DS), polystyrene sulfonate (PSS), and polymethylacrylate (PMA). Expressed in terms of polyion segments, the concentrations of the polyelectrolytes are in the range of 0.001-0.01 molal. The monovalent counterion concentrations are in the range of 0.002-0.02 molal, while the divalent counterion concentrations are even smaller, in the range of 1.7e-5 to 0.008 molal. Unless specifically indicated in this paper, the temperature is 298.15 K.

It should be noted that the lc term has little contribution to the system nonideality at the exceedingly low counterion concentrations of the literature data examined in this study. Therefore, this study only considers the Manning term and the PDH term, the binary interaction parameters τ_{ij} of the lc term has been set to zero, and the only adjustable model parameter is ξ for each polyelectrolyte. In this work, the ξ parameter is identified by minimizing the following objective function,

$$\text{Objective Function} = \sum_{j=1}^N \left(\frac{x_j^{\text{calc}} - x_j^{\text{expt}}}{\sigma_x} \right)^2, \quad (17)$$

Here j is the data point index, N is the total number of data points in the data set, the superscripts “calc” and “expt” are for the model results and the experimental data, respectively. σ_x is the assumed standard deviation for the experimental data, set to 5%. The average relative deviation in percentage (ARD %) is used to evaluate the quality of data fitting.

$$ARD\% = 100 \times \frac{1}{N} \sum_{j=1}^N \left| \frac{x_j^{calc} - x_j^{expt}}{x_j^{expt}} \right|, \quad (18)$$

4. Results and Discussion

Figure 2 to Figure 7 show the comparison between the selected experimental data from multiple sources [14-17, 19] and the corresponding model results. Table 3 presents the identified Manning parameter ξ values from the regression and the associated ARD% for DBT and mDBT. It should be noted that the ξ value is independent of counterions and the same ξ value is reported for each polyion from each data source.

Figure 2 shows a comparison between the model results and the experimental data of the polyion condensation fraction of Mg^{2+} for the Na^+ - Mg^{2+} -DS system [14] with $m_{p,0} = 0.001$ molal and a total added salt concentration (expressed as ionic strength) of 0.01 molal. The model results from DBT and mDBT are shown as dashed and solid lines, respectively. Both models represent well the polyion condensation fraction of Mg^{2+} in the system. The model results with mDBT show a slight improvement over the DBT results, reflecting the fact that the contribution of the additional g^{PDH} term to DBT is minor at low concentrations. To examine the selectivity of counterions condensing on the polyion chain, the degree of condensation in % for each counterion is also calculated and shown in Figure 2. The degree of condensation for counterion i (η_i) is defined as the ratio of the condensed counterion amount over the total counterion amount in the system:

$$\eta_i(\%) = n_i^c / n_i^{tot} \times 100, \quad (19)$$

where n_i^c is the amount of condensed counterion i , and n_i^{tot} is the total amount of counterion i . Indicative of the high selectivity of Mg^{2+} condensation over Na^+ condensation, the highest degree of Mg^{2+} condensation was observed in the region with low Mg^{2+} concentration. Upon increasing Mg^{2+} concentration, the polyion condensation fraction of Mg^{2+} $\theta_{Mg^{2+}}$ increases, and the degree of Mg^{2+} condensation $\eta_{Mg^{2+}}$ decreases correspondingly. Similar results were observed in the other three DS systems listed in Table 3.

Figure 3 shows the model correlation results for the polyion condensation fractions of individual counterion for the Na^+ - Pb^{2+} -PSS system [15]. The concentration of the polyion segment was fixed at 0.001 molal, and the total ionic strength of the added salt was fixed at 0.01 molal. The experimental results showed that, as the concentration of Pb^{2+} increases, $\theta_{Pb^{2+}}$ increases, θ_{Na^+} decreases, and $\eta_{Pb^{2+}}$ decreases. Again, the mDBT results show slight improvement over the DBT results. The divalent counterion Pb^{2+} is favorable for condensation on polyions by a factor of ~ 10 when compared with the monovalent counterion Na^+ in this system.

Figure 4 shows a comparison between the model results and the experimental data of the polyion condensation fraction for Na^+ and Ca^{2+} in the PMA solution [16]. The concentration of polyion was fixed at 0.002 molal, and the concentration of Na^+ was fixed at 0.002 molal. Similar trends of polyion condensation fractions were observed for this polyelectrolyte system. At low Ca^{2+} concentration, the degree of condensation for Ca^{2+} is 100%. With increasing Ca^{2+} concentration, the polyion condensation fraction of Ca^{2+} increases and the polyion condensation fraction of Na^+ drops. The Ca^{2+} selectivity over the Na^+ selectivity is overwhelming, in terms of the degree of condensation of individual ion. Due to the overall very low salt concentration, the DBT and mDBT model results are almost identical.

Figure 5 and Figure 6 show the comparison of the experimental data [19] and the model results for the activity coefficients of Mg^{2+} and Ca^{2+} for the Na^+ - Mg^{2+} -DS and Na^+ - Ca^{2+} -DS systems, respectively. The concentration of polyion was fixed at 0.001 molal. The total added salt concentration in terms of ionic strength was 0.015 molal for the Na^+ - Mg^{2+} -DS system and 0.005 molal for the Na^+ - Ca^{2+} -DS system. In Figure 5a, the model results show good agreement with the experimental data of activity coefficient of Mg^{2+} for the Na^+ - Mg^{2+} -DS system, and there is no significant difference in the DBT results and the mDBT results. Figure 5b presents the corresponding model results for the polyion condensation fractions and the degrees of condensation. With an increase in the concentration of Mg^{2+} , the polyion condensation fraction of Mg^{2+} increases, while that of Na^+ decreases. In addition, Mg^{2+} is the strongly preferred counterion for condensation. Similarly, in Figure 6a, the model represents well the experimental data for activity coefficient of Ca^{2+} for the Na^+ - Ca^{2+} -DS system, and Figure 6b suggests high selectivity for Ca^{2+} over Na^+ .

Figure 7a presents the model results and the experimental data for activity coefficients of counterions for the Na^+ - Mg^{2+} -PSS system [17]. The concentration of the polyion was 0.01 molal. Na^+ , as the counterion of the polyelectrolyte, is at an equivalent concentration of 0.01 molal. The divalent counterion, Mg^{2+} , was introduced as added salt ($MgCl_2$) at various concentrations from $8e-4$ to $8e-3$ molal. With the Manning parameter ξ as the only adjustable parameter, the model results agree well with the experimental data for both Na^+ and Mg^{2+} activity coefficients. The corresponding polyion condensation fraction and the degree of condensation are shown in Figure 7b. The mDBT model results suggest that the polyion condensation fraction of Mg^{2+} increases and the degree of condensation of Mg^{2+} decreases with increased Mg^{2+} concentration in the solution. Furthermore, the selectivity of Mg^{2+} condensation is higher than that of Na^+ by a factor

of ~3, although the selectivity of Mg^{2+} over Na^+ declines with increasing Mg^{2+} concentration in the solution.

5. Conclusions

Incorporating a modified Delocalized Binding Theory for counterion condensation, the polyelectrolyte NRTL model was successfully applied to correlate experimental measurements of polyion condensation fractions and activity coefficients of aqueous polyelectrolyte solutions with mixed monovalent and divalent counterions. Consistent with experimental observation, the model suggests that counterions with high valence have higher polyion condensation fractions and therefore higher selectivity as condensed species especially in the low salt concentration region. Although only validated for data at low salt concentrations due to availability of data, the polyelectrolyte NRTL model has been shown to be a comprehensive thermodynamic model for aqueous polyelectrolyte solutions with mixed-valent counterions. Future work will focus on the application of the model to study mobile ion partitioning in ion-exchange membranes immersed in saline solutions with mixed-valent salts.

Acknowledgments

Funding support was provided by the U. S. Department of Energy under the grant DE-EE0007888. The authors gratefully acknowledge the financial support of the Jack Maddox Distinguished Engineering Chair Professorship in Sustainable Energy sponsored by the J.F. Maddox Foundation.

Disclaimer

This report was prepared as an account of work sponsored by an agency of the United States Government. Neither the United States Government nor any agency thereof, nor any of

their employees, makes any warranty, express or implied, or assumes any legal liability or responsibility for the accuracy, completeness, or usefulness of any information, apparatus, product, or process disclosed, or represents that its use would not infringe privately owned rights. Reference herein to any specific commercial product, process, or service by trade name, trademark, manufacturer, or otherwise does not necessarily constitute or imply its endorsement, recommendation, or favoring by the United States Government or any agency thereof. The views and opinions of authors expressed herein do not necessarily state or reflect those of the United States Government or any agency thereof.

References

- [1] S. Lifson, A. Katchalsky, The Electrostatic Free Energy of Polyelectrolyte Solutions. II. Fully Stretched Macromolecules, *J. Polym. Sci.*, 13 (1954) 43-55.
- [2] F. Oosawa, A Simple Theory of Thermodynamic Properties of Polyelectrolyte Solutions, *J. Polym. Sci.*, 23 (1957) 421-430.
- [3] G.S. Manning, B.H. Zimm, Cluster Theory of Polyelectrolyte Solutions. I. Activity Coefficients of the Mobile Ions, *J. Chem. Phys.*, 43 (1965) 4250-4259.
- [4] G.S. Manning, Limiting Laws and Counterion Condensation in Polyelectrolyte Solutions I. Colligative Properties., *J. Chem. Phys.*, 51 (1969) 924-933.
- [5] M. Rinaudo, M. Milas, Activity Coefficients of Small Ions in Aqueous Mixtures of Polyelectrolytes and Simple Electrolytes, *Chem. Phys. Lett.*, 41 (1976) 456-459.
- [6] Y. Yu, Y. Li, N. Hossain, C.-C. Chen, Modeling of Polyelectrolytes System with Electrolyte Nonrandom Two-Liquid Model, *Fluid Phase Equilib.*, 497 (2019) 1-9.
- [7] Y. Li, Y. Yu, C.-C. Chen, Modeling Aqueous Multivalent Polyelectrolytes Systems with Polyelectrolyte Nrtl Model, *J. Mol. Liq.*, (2021) 116237.
- [8] K.S. Pitzer, Electrolytes. From Dilute Solutions to Fused Salts, *Journal of the American Chemical Society*, 102 (1980) 2902-2906.
- [9] C.-C. Chen, B. Evans, Thermodynamic Representation of Phase Equilibria of Mixed-Solvent Electrolyte Systems, *AIChE Journal*, 32 (1986) 1655-1664.
- [10] Y. Song, C.-C. Chen, Symmetric Electrolyte Nonrandom Two-Liquid Activity Coefficient Model, *Ind. Eng. Chem. Res.*, 16 (2009) 7788-7797.
- [11] Y. Yu, N. Yan, B.D. Freeman, C.-C. Chen, Mobile Ion Partitioning in Ion Exchange Membranes Immersed in Saline Solutions, *J. Membr. Sci.*, 620 (2021) 118760.
- [12] G.S. Manning, Limiting Laws for Equilibrium and Transport Properties of Polyelectrolyte Solutions, in: E. Sélégny, M. Mandel, U.P. Strauss (Eds.) *Polyelectrolytes: Papers Initiated by a Nato Advanced Study Institute on Charged and Reactive Polymers Held in France, June 1972*, Springer Netherlands, Dordrecht, 1974, pp. 9-37.
- [13] G.S. Manning, The Molecular Theory of Polyelectrolyte Solutions with Applications to the Electrostatic Properties of Polynucleotides, *Q. Rev. Biophys.*, 11 (1978) 179-246.
- [14] Y.M. Joshi, J.C.T. Kwak, The Binding of Divalent Metal Ions to Polyelectrolytes in Mixed Counterion Systems: II. Dextran sulfate-Mg²⁺ and Dextran sulfate-Ca²⁺ in Solutions Containing Added NaCl or KCl, *Biophys. Chem.*, 13 (1981) 65-75.
- [15] E. Nordmeier, W. Dauwe, Studies of Polyelectrolyte Solutions I. Counterion Condensation by Poly(styrene sulfonate), *Polym. J.*, 23 (1991) 1297-1305.
- [16] J. C. Benegas, S. Paoletti, A. Cesàro, M.A.G.T. van den Hoop, H.P. van Leeuwen, Limiting-Laws of Polyelectrolyte Solutions. Ionic Distribution in Mixed-Valency Counterions Systems. II A Comparison of Conductometric Data and Theoretical Predictions, *Biophys. Chem.*, 42 (1992) 297-303.
- [17] M. Satoh, T. Kawashima, J. Komiyama, A New Model of Counterion Condensation in Polyelectrolyte Solutions: III. Theoretical Predictions of Competitive Condensation between Counterions of Different Valences, *Biophys. Chem.*, 31 (1988) 209-215.
- [18] K.S. Pitzer, G. Mayorga, Thermodynamics of Electrolytes. II. Activity and Osmotic Coefficients for Strong Electrolytes with One or Both Ions Univalent, *J. Phys. Chem.*, 77 (1973) 2300-2308.
- [19] J.C.T. Kwak, Y.M. Joshi, The Binding of Divalent Metal Ions to Polyelectrolytes in Mixed Counterion Systems: I. The Dye Spectrophotometric Method, *Biophys. Chem.*, 13 (1981) 55-64.
- [20] Y. Yan, C.-C. Chen, Thermodynamic Representation of the NaCl-Na₂SO₄-H₂O System with Electrolyte NRTL Model, *Fluid Phase Equilib.*, 306 (2011) 149-161.

- [21] S. Tanveer, C.-C. Chen, Thermodynamic Modeling of Aqueous Ca^{2+} - Na^+ - K^+ - Cl^- Quaternary System, *Fluid Phase Equilib.*, 409 (2016) 192-206.
- [22] S. Tanveer, H. Zhou, C.-C. Chen, Thermodynamic Model of Aqueous Mg^{2+} - Na^+ - K^+ - Cl^- Quaternary System, *Fluid Phase Equilib.*, 437 (2017) 56-68.

Figure Legend

Figure 1. Contour plots of Gibbs energy contribution for Delocalized Binding Theory with varying θ_1 for monovalent and θ_2 for divalent counterions for a polyelectrolyte system with $\xi = 2.5$, $m_{p,0} = 0.01$, $m_{1,0} = 0.01$, and $m_{2,0} = 0.01$ molal. (a) Total Gibbs energy; (b) g^{el} ; (c) g^{mix}

Figure 2. Comparison between experimental data [14] and model correlation results of polyion condensation fractions (θ_i) for the Na^+ - Mg^{2+} -DS system with a polyion concentration ($m_{p,0}$) of 0.001 molal and total ionic strength for added salts (I) of 0.01 molal. The regressed parameter ξ is 2.42 for DBT and 2.79 for mDBT.

Figure 3. Comparison between experimental data [15] and model correlation results of polyion condensation fraction (θ_i) for the Na^+ - Pb^{2+} -PSS system with polyion concentration ($m_{p,0}$) of 0.001 molal and total ionic strength for added salts (I) of 0.01 molal. The regressed parameter ξ is 2.42 for DBT and 2.70 for mDBT.

Figure 4. Comparison between experimental data [16] and model correlation results of counterion condensation fraction (θ_i) for the Na^+ - Ca^{2+} -PMA system with polyion concentration ($m_{p,0}$) of 0.002 molal and Na^+ concentration ($m_{\text{Na}^+,0}$) of 0.002 molal. The regressed parameter ξ is 2.29 for DBT and 2.31 for mDBT.

Figure 5. Model correlation results for the Na^+ - Mg^{2+} -DS system with polyion concentration ($m_{p,0}$) of 0.001 molal and salt concentration in the form of ionic strength $I = 0.015$ molal. [19] (a) Counterion activity coefficient (γ_i), and (b) counterion condensation fraction (θ_i) and degree of condensation (η_i). The regressed parameter ξ is 2.28 for DBT and 2.45 for mDBT.

Figure 6. Model correlation results for the Na^+ - Ca^{2+} -DS system with a polyion concentration ($m_{p,0}$) of 0.001 molal and salt concentration in the form of ionic strength $I = 0.005$ molal. [19] (a) Counterion activity coefficient (γ_i), and (b) counterion condensation fraction (θ_i) and degree of condensation (η_i). The regressed parameter ξ is 2.28 for DBT and 2.45 for mDBT.

Figure 7. Model correlation results for the Na^+ - Mg^{2+} -PSS systems with a polyion concentration ($m_{p,0}$) of 0.01 molal and Na^+ concentration ($m_{\text{Na}^+,0}$) of 0.01 molal. [17] (a) Counterion activity coefficient (γ_i), and (b) counterion condensation fraction (θ_i) and degree of condensation (η_i). The regressed parameter ξ is 1.94 for DBT and 2.08 for mDBT.

Figures

Figure 1.

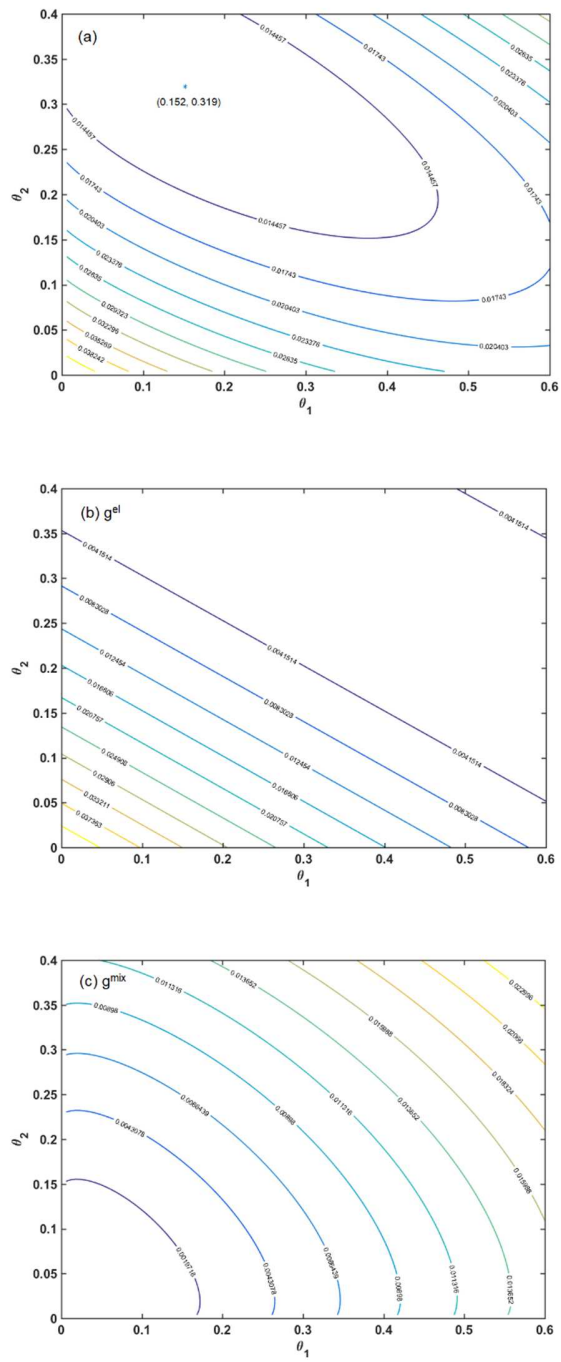


Figure 2.

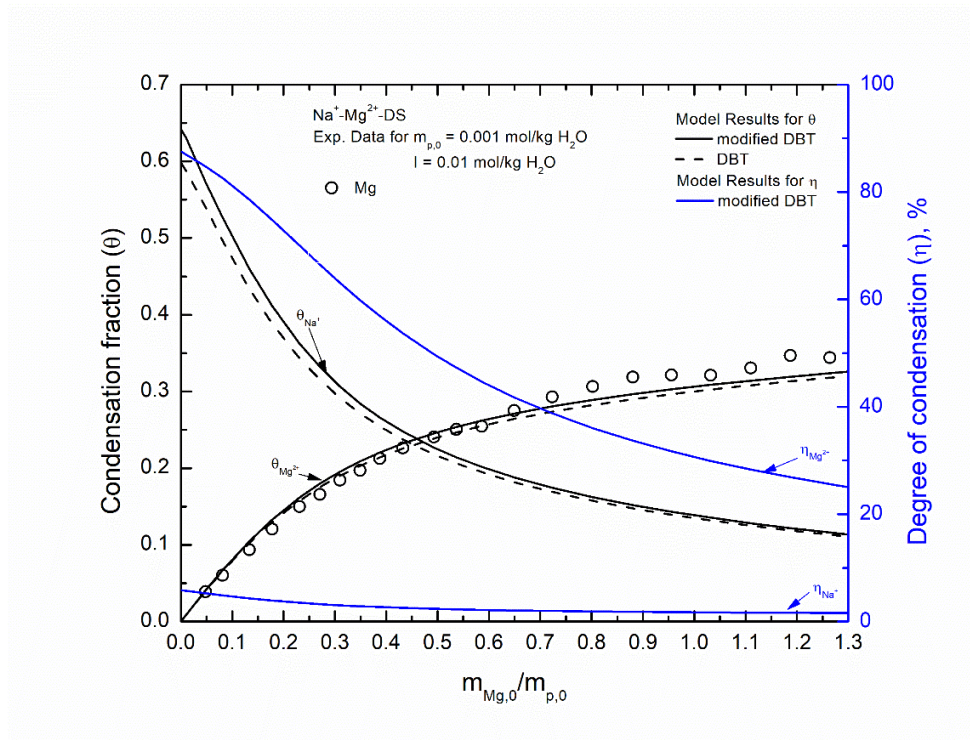


Figure 3.

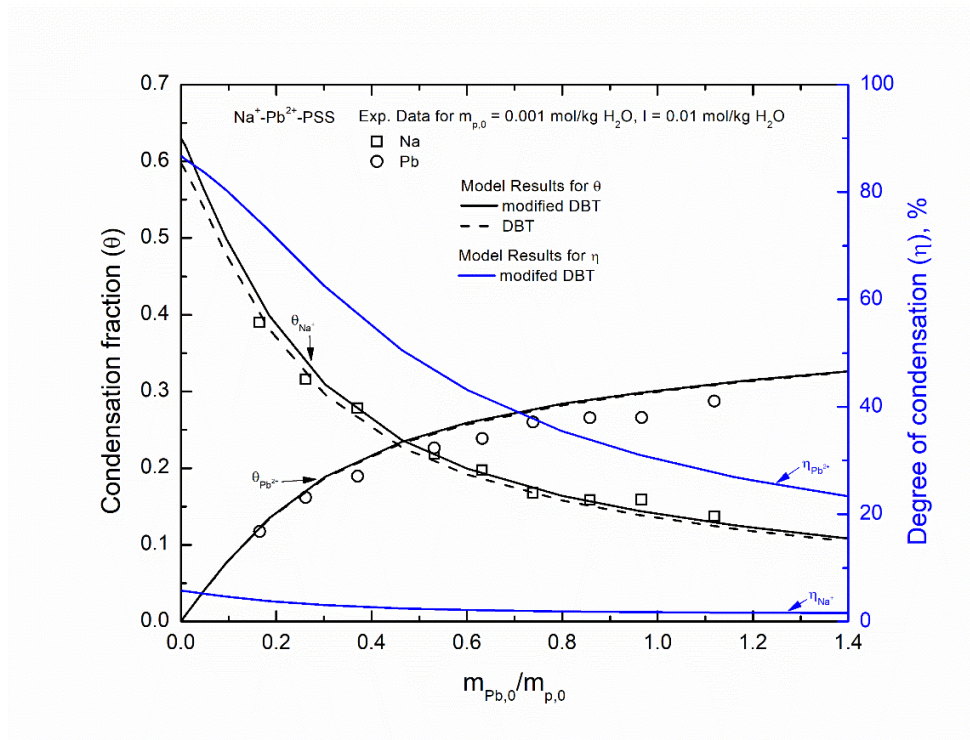


Figure 4.

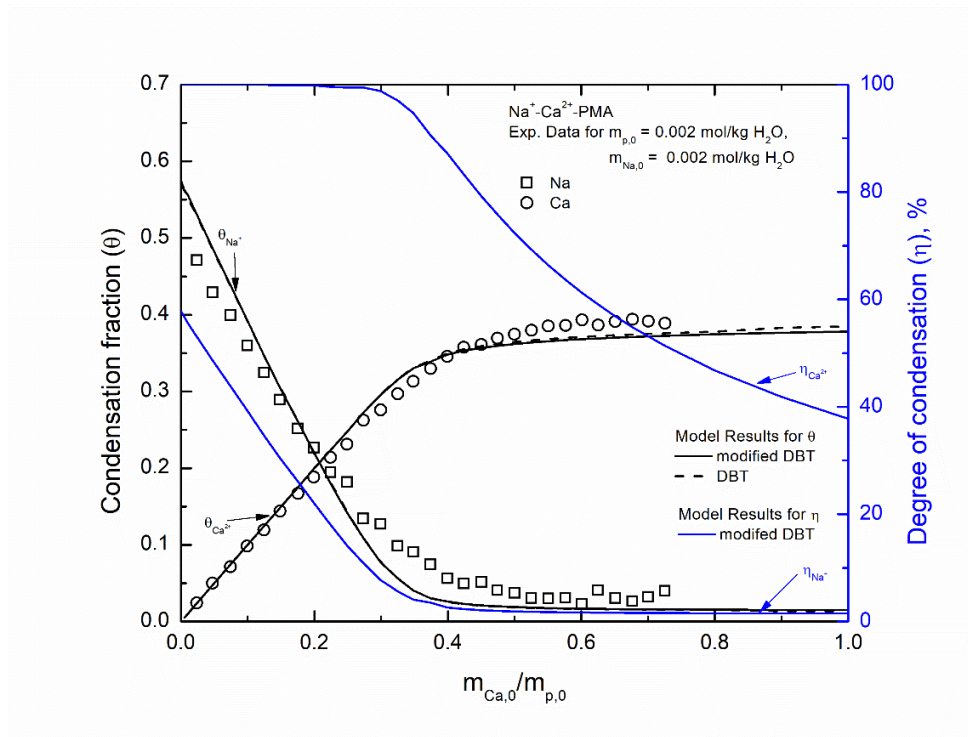


Figure 5.

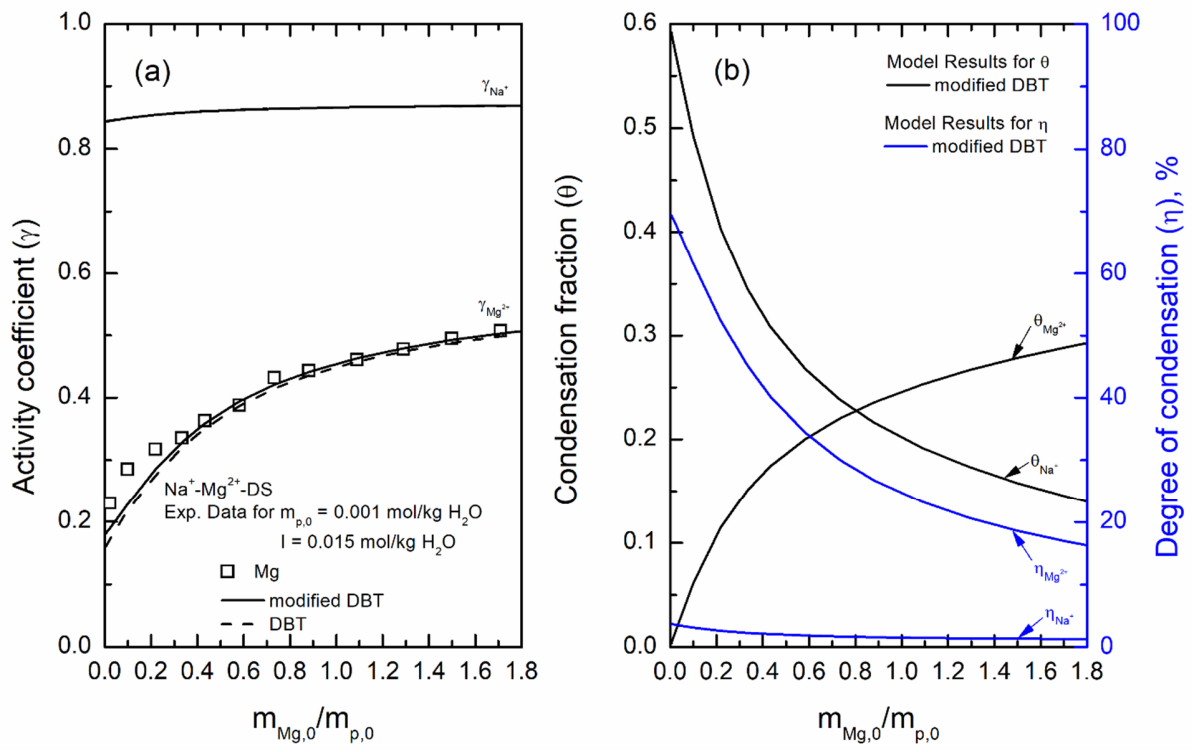


Figure 6.

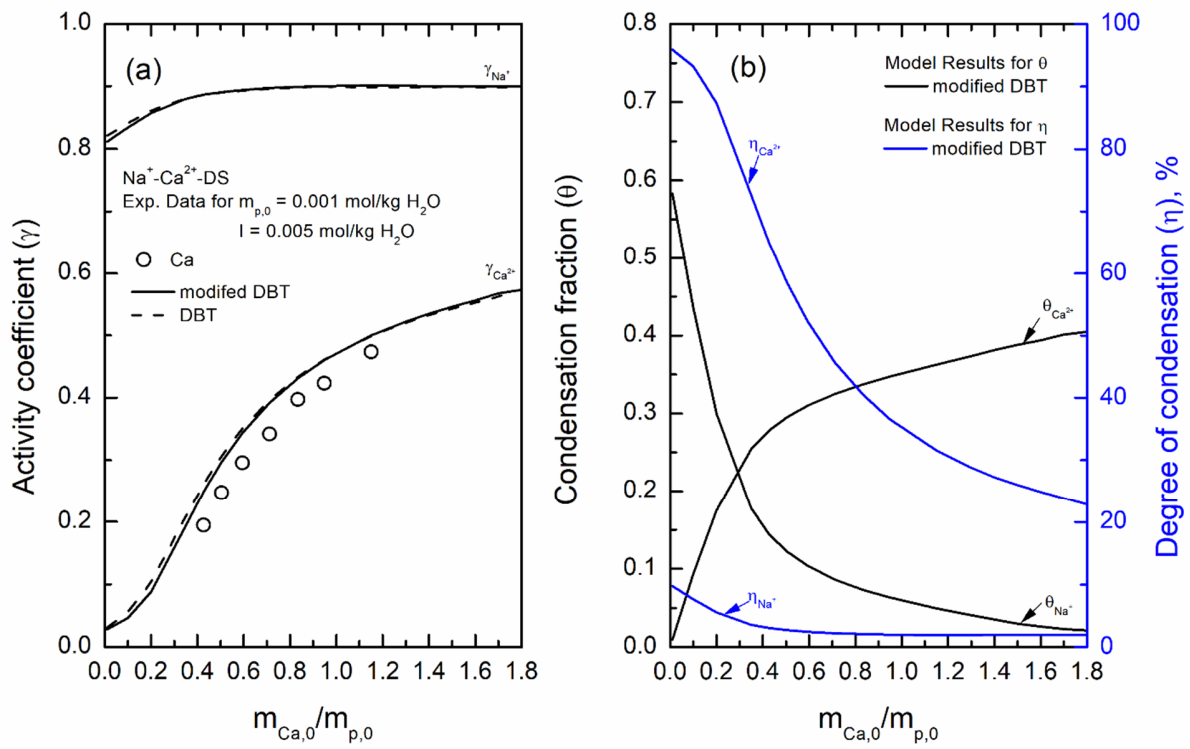
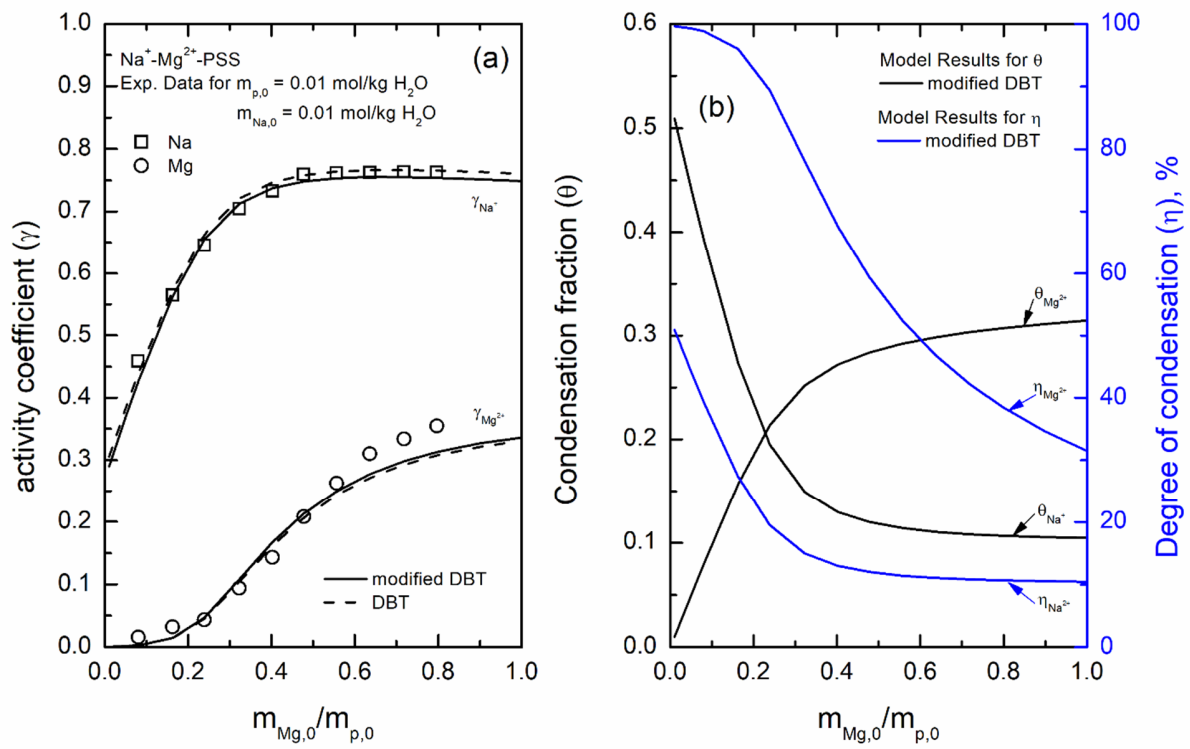


Figure 7.



Tables

Table 1. Polyelectrolyte NRTL Model Parameters for Each Contribution Term

Contribution term		Parameter	Source
Manning term		ξ	This study
PDH term		None	n.a.
lc term	water-electrolyte pair for simple electrolytes like alkali halides	τ_{ij}	Literatures*
	water-electrolyte pair for ion pairs involving polyion charged segments and counterions	τ_{ij}	Set to zero in this study
	electrolyte-electrolyte pair	τ_{ij}	Set to zero in this study

* The eNRTL binary interaction parameters for water-electrolyte pairs are readily available in published literatures for most common electrolytes such as NaCl [20], CaCl₂ [21], MgCl₂ [22], etc.

Table 2. Literature data of polyelectrolyte solutions with mixed-valent counterions

Source	Data type	Polyion	$m_{polyion}$	Counterions	m_{M^+}	$m_{M^{2+}}$	Coion	No. of date points
Joshi and Kwak (1981) [14]	$\theta_{M^{2+}}$	DS	0.001 – 0.01	Na ⁺ , Mg ²⁺	0.0037–0.055	1.8e-5–0.0065	Cl ⁻	219
			0.001	Na ⁺ , Ca ²⁺	0.0023–0.011	9.7e-5–0.0013		41
			0.001	K ⁺ , Mg ²⁺	0.0035–0.011	2e-5–0.0013		47
			0.001	K ⁺ , Ca ²⁺	0.0035–0.011	1.7e-5–0.0012		44
Nordmeier and Dauwe (1991) [15]	$\theta_{M^+}, \theta_{M^{2+}}$	PSS	0.001-0.006	H ⁺ , Pb ²⁺	0.01, 0.02	1e-4–0.0012	NO ₃ ⁻	36
				Na ⁺ , Pb ²⁺	0.01, 0.02	1.6e-4–0.0011		38
Benegas <i>et al.</i> (1992) [16]	$\theta_{M^+}, \theta_{M^{2+}}$	PMA	0.002	Na ⁺ , Mg ²⁺	0.002	4.7e-4–0.0015	NO ₃ ⁻	58
				Na ⁺ , Ca ²⁺	0.002	4.5e-4–0.0014		58
Kwak and Joshi (1981) [19]	$\gamma_{M^{2+}}$	DS	0.001	Na ⁺ , Mg ²⁺	0.01–0.016	2.2e-5–0.0017	Cl ⁻	15
				Na ⁺ , Ca ²⁺	0.002–0.005	4.3e-4–0.0012		17
Satoh <i>et al.</i> (1988) [17]	$\gamma_{M^+}, \gamma_{M^{2+}}$	PSS	0.01	Na ⁺ , Mg ²⁺	0.01	8e-4–0.008	Cl ⁻	20
				Na ⁺ , Ca ²⁺	0.01	8e-4–0.008		20

* Unit of concentration is molality

Table 3. Regressed model parameters of polyelectrolyte NRTL model for polyelectrolyte solutions with mixed-valent counterions

Systems	Parameters		ARD%, DBT	ARD%, mDBT	Data source
	ξ , DBT	ξ , mDBT			
Na ⁺ -Mg ²⁺ -DS	2.42±0.06	2.79±0.02	12.54	8.07	Joshi and Kwak (1981) [14]
Na ⁺ -Ca ²⁺ -DS			10.02	7.84	
K ⁺ -Mg ²⁺ -DS			23.03	19.78	
K ⁺ -Ca ²⁺ -DS			11.38	13.50	
Na ⁺ -Pb ²⁺ -PSS	2.42±0.01	2.70±0.23	4.90	3.10	Nordmeier and Dauwe (1991) [15]
H ⁺ -Pb ²⁺ -PSS			13.39	14.41	
Na ⁺ -Mg ²⁺ -PMA	2.29±0.02	2.31±0.02	23.81	23.84	Benegas <i>et al</i> (1992) [16]
Na ⁺ -Ca ²⁺ -PMA			18.94	18.94	
Na ⁺ -Mg ²⁺ -DS	2.28±0.13	2.45±0.12	6.65	4.77	Kwak and Joshi (1981) [19]
Na ⁺ -Ca ²⁺ -DS			14.59	12.76	
Na ⁺ -Mg ²⁺ -PSS	1.94±0.04	2.08±0.24	11.25	11.64	Satoh <i>et al.</i> (1988) [17]
Na ⁺ -Ca ²⁺ -PSS			13.40	13.50	